chemosensors

MDPI

Article

Optimization of a Handwriting Method by an Automated Ink Pen for Cost-Effective and Sustainable Sensors

Florin C. Loghin [1], José F. Salmerón [2], Paolo Lugli [3], Markus Becherer [1], Aniello Falco [3] and Almudena Rivadeneyra [2,*]

[1] Institute for Nanoelectronics, Technical University of Munich, 80333 Munich, Germany; florin.loghin@tum.de (F.C.L.); markus.becherer@tum.de (M.B.)
[2] Pervasive Electronics Advanced Research Laboratory (PEARL), Department of Electronics and Computer Technology, University of Granada, 18071 Granada, Spain; jfsalmeron@ugr.es
[3] Faculty of Science and Technology, Free University of Bolzano, 39100 Bolzano, Italy; paolo.lugli@unibz.it (P.L.); aniello.falco@unibz.it (A.F.)
* Correspondence: arivadeneyra@ugr.es; Tel.: +34-958248996

Abstract: In this work, we present a do-it-yourself (DIY) approach for the environmental-friendly fabrication of printed electronic devices and sensors. The setup consists only of an automated handwriting robot and pens filled with silver conductive inks. Here, we thoroughly studied the fabrication technique and different optimized parameters. The best-achieved results were 300 mΩ/sq as sheet resistance with a printing resolution of 200 µm. The optimized parameters were used to manufacture fully functional electronics devices: a capacitive sensor and a RFID tag, essential for the remote reading of the measurements. This technique for printed electronics represents an alternative for fast-prototyping and ultra-low-cost fabrication because of both the cheap equipment required and the minimal waste of materials, which is especially interesting for the development of cost-effective sensors.

Keywords: additive manufacturing; ball pen; flexible substrate; printed electronics; silver nanoparticles

Citation: Loghin, F.C.; Salmerón, J.F.; Lugli, P.; Becherer, M.; Falco, A.; Rivadeneyra, A. Optimization of a Handwriting Method by an Automated Ink Pen for Cost-Effective and Sustainable Sensors. *Chemosensors* **2021**, *9*, 264. https://doi.org/10.3390/chemosensors9090264

Academic Editor: Yu-Ting Cheng

Received: 25 June 2021
Accepted: 11 September 2021
Published: 16 September 2021

1. Introduction

The development of the Internet of Things (IoT) has created a surge in the request of electronic sensing or communicating notes. Inevitably, however, to reach the mass market, while keeping in sight the targets of economic and environmental sustainability, it will be necessary to produce low-cost devices and to minimize the waste of raw material and non-recyclable final products. In addition to this, new requirements, which could expand the fields of application of IoT nodes, have attracted the attention of end-users, such as flexibility, light-weight, and biocompatibility [1,2]. In this novel framework, innovative manufacturing techniques and new materials are becoming more and more popular. In particular, printed electronics (PE) and handwriting electronics (HWE) are gaining momentum. The former refers to traditional printing techniques, such as inkjet printing, screen printing, and gravure, applied to electronic circuit design [3–5]. The latter is based on handwriting techniques, such as a brush pen or ball pen, to build electronic devices [6].

In the past decade, PE has significantly developed in the field of sensors [7–9] and radiofrequency identification (RFID) technology [10,11]. The main advantages with respect to traditional clean room processes are the lower cost of the equipment, the operating conditions, and the speed of prototyping, among others. Especially interesting are final applications where no silicon-based element is included but only printed ones to build a functional system. Other examples of PE are harvesters and logic circuits. Ishida et al. developed a piezoelectric energy harvester together with the pedometer circuit; the pseudo-CMOS 14-bit step counter is able to record up to 16,383 steps using the harvested power [12]. Moreover, Chang et al. described analogue and mixed-signal circuits, including differential amplifiers, and a charge-redistribution 4-bit digital-to-analogue converter (DAC) [13].

Recently, HWE has awaken the interests of researcher because it can provide the same benefits as PE but its cost are even smaller, facilitating prototyping and allowing do-it-yourself (DIY) electronics [6]. Different writing techniques, such as pencil [14,15], brush pen [16], ball pen [17,18], and fountain pen [19,20] have been lately employed to directly define electronic circuits. For example, commercial pencils have been utilized for ultraviolet (UV) sensors [21,22] and photodetectors [23]. Further, custom-made pencils based on carbon nanomaterials have been developed for gas sensing applications [24,25]. The drawback of this technology is its poor resolution and lack of reproducibility limited by human eye and freehand lines, which constituted the main bottleneck for the commercial development of this technology.

Brush and rollerball pens have been already employed with metal inks to develop circuits interconnects and passive electronic components (capacitors, resistors and inductors) as well as to combine them into simple circuitry [16,26]. Even handwriting techniques have been already used to develop antennas at different operating frequencies [27,28]. Further, by utilizing these techniques, different kind of sensors have been fabricated. For example, Li et al. directly wrote with a rollerball pen glucose sensors based on carbon- and sliver-based conductive materials [29]. Kano et al. fabricated a flexible respiration sensor to detect relative humidity (RH) by defining graphite electrodes with a pencil and depositing an RH sensitive layer based on silica nanoparticles using a brush pen-sensitive silica NP film [30]. Yu et al. designed a skin circuit for biosignal acquisition based on this technology. In particular, they were able to record the electrocardiogram (ECG) [31].

However, although all these examples demonstrate the potential of handwriting technology to create electronics components, they lack of reproducibility and the resolution of the written patterns is very poor. In this direction, some efforts have been devoted to open more possibilities to handwriting electronics by using pen analogues and writing machines [32]. For example, Soum et al. presented an automated HWE system based on ball pens and a plotter robot [33]. They described the fabrication method and its applicability to develop disposable electrochemical sensor. However, they did not show which parameters of the system affect the electrical and physical properties of the written electronics.

The fabrication process we describe and characterize in this work tackles these two main issues and conjugates the inherent simplicity of HWE with the precision of computer control. In particular, we report the optimization of an automated ball pen to write electronics pointing out the parameters that influence the fabrication with such technique and the optimal manufacturing parameters for a common employed ink in PE. Finding the most suitable writing parameters is of paramount importance to guarantee sufficient stability and reproducibility of processing conditions. These elements are crucial in the realization of any electronic device, and even more in the constantly growing field of printed sensors. To showcase the potential of the technique, after finding the most satisfactory parameters, we employ it to create two sets of electronic components: passive gas sensors and the RFID tags essential to build sensor systems with remote readout.

2. Materials and Methods

2.1. Manufacturing Process

The AxiDraw robot is a precise and versatile pen plotter; it is normally used to create for example postcards, invitations, or drawings. The vector graphic program Inkscape, extended with the official AxiDraw plugin, is used to control it. First, the setup of the pen needs to be adjusted. Therefore, the height in the up and down position is set, so that the pen touches the surface when down low and raises high enough not to write accidentally when moving around without the intention to distribute ink. Alongside the height, the writing and raising speed can be set and a delay after the raising and lowering of the pen can be added. When all the regulations are finished, the writing process can be started by the plot command. In order to obtain satisfying results, a number of different pens, as well as varying substrates, have been investigated. This section describes the methods and

actions that were performed within this work, including both, the handwritten tests, and primarily the writings executed by the AxiDraw robot.

In this work, we tested a silver nanoparticle (AgNP) ink from ANP (DGP-40LT-15C), containing 30–35%wt nanoparticles in triethylene glycol monomethyl ether (TGME). The particles size was at maximum 50 nm. The writing process was performed at normal environmental conditions.

Firstly, we tested three different types of pens to determine the most suitable to obtain reproducible silver pattern: nibs, gel pens, and ball pens. The best tests results were found for ball pens. The handwriting tests showed quite uniform lines, especially compared to the other tested pens. The drawback of this option is the tip degradation over time. When non-printing, the ink slightly dries on the pen's tip, causing its blocking. Storing the pen in the fridge with the tip pointing upwards helps with this issue. Printing some dummy designs before the printing enhances the results significantly. In particular, we employed a Cartridge-Rollerball-System with a 0.7 mm TC ball fabricated by Schmidt technology (see Figure 1a). Once the pen was selected, we performed tests with different layouts on photopaper as it is shown in Section 3. The selected substrate was EMBLEM Poster Paper with 200 g/m^2 weight (SOPEP200).

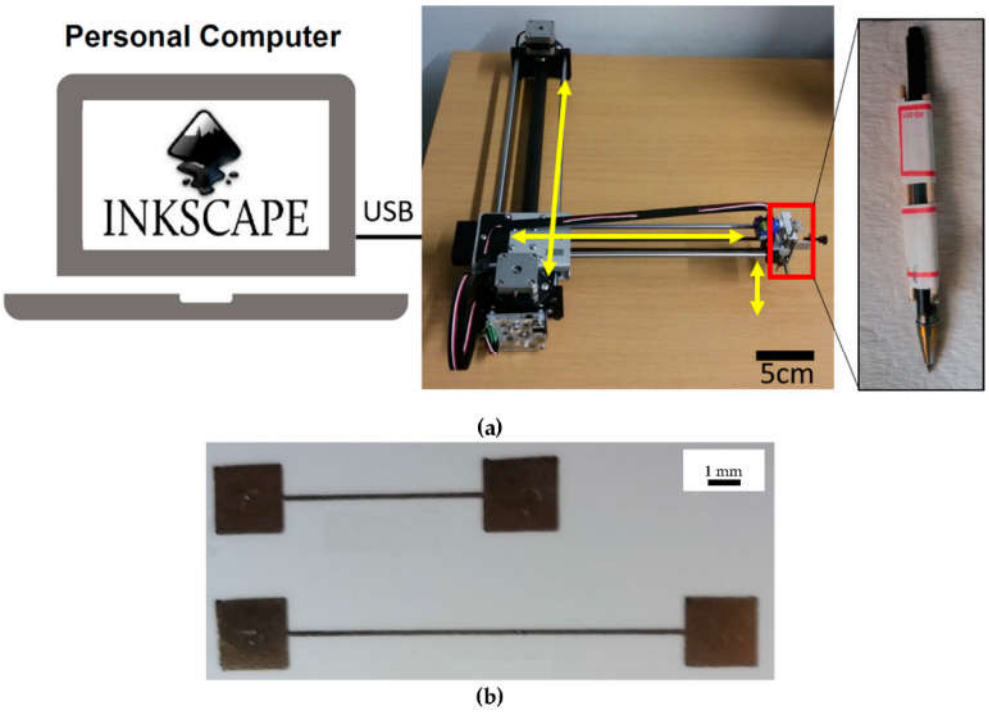

Figure 1. (**a**) General setup of HWE system. Shown is a schematic of the software (Inkscape) connected to an automated XY-Stage in which a ballpoint is fixated. (**b**) Written layout.

Therefore, to study the influence of the speed in the resolution, we resorted to a safer option and set lines of 250 µm width (Figure 1b), while checking the process quality at 5 different speeds: 10 mm/s, 25 mm/s, 50 mm/s, 75 mm/s, and 100 mm/s. We took microscope images of lines at the different speeds, digitized them, and converted their edges to numerical data. This information was used to estimate the average width, its standard deviation, the standard deviation of the single edges and their ratio to the width.

After the writing of the patterns, the AgNPs were photonically sintered with a Sinteron 2010 (Xenon Corporation, Wilmington, MA, USA). Following the results of the optimization of sheet resistance for the same silver ink [34], we used a pulse width of 500 µs and a periodicity of 1 s for 15 times at 2.1 W.

2.2. Characterization

For electrode morphology characterization, scanning electron microscopy (SEM) was performed. SEM-images were recorded with a field-emission scanning electron microscope (NVision40 from Carl Zeiss AG, Oberkochen, Germany) at an extraction and acceleration voltage of 5 and 7 kV, respectively. To optimize the image quality, the working distance was adjusted in the range 5–6 mm. White light interferometer (WLI) images were recorded using a NT9080 from Veeco (Plainview, NY, USA)

Optical microscope images (DM 2500 equipped with a DFC295 camera, both of Leica Microsystems (Germany)) were taken for visual inspection of the written patterns. The sheet resistance of the conductive layers was measured with using a four-point probe head from Jandel connected to a source-measuring unit (Keysight B2901A).

3. Results

3.1. Speed and Resolution

To fully characterize the technique, we started with the analysis of the effect of the speed of the arm robot on the quality of the written pattern, as well as the resolution achieved when defining lines and squares/corners. Such parameters are crucial to define electrodes, sensing layers among others electronic components. For example, the sensitivity of capacitive sensors is directly related to de geometry of the electrodes; in the case of interdigitated electrodes (IDEs) employed in planar capacitive sensors, the closer the fingers are the higher the sensitivity results. It should be noted that the pen was in contact with the paper with no additional weight while writing the patterns to reduce the process parameters and keep the setup as simple as possible. Our observations show that although lines narrower than 200 µm can be written, the likelihood for failures increases, especially for what concerns the straightness of the lines. To enhance the achieved resolution, it a pen with a smaller tip would be required.

The most representative information for this study is certainly the mean width and its standard deviation, which are detailed in Table 1. It can be seen in Figure 2 that the higher the speed is then the narrower the lines are. There is a variation in the width of about 65 µm between the 10 mm/s and the 100 mm/s, with the biggest part of the change happening in the first step (10 mm/s to 25 mm/s). This can be associated with the fact that higher speed deposits less material than slower ones, however, as long as the minimum flow of material that guarantees a continuous line is kept, the width does not deviate significantly from the target value. In absolute terms, the width value closer to the target one was obtained with 25 mm/s, however the resulted line is wavier. The more straight lines resulted with a fabrication speed of either 10 mm/s or 100 mm/s, although they deviated significantly from the target. The best compromise between straightness and width is found for 75 mm/s, which is only marginally better than the other options and offers the additional benefit of quicker writing speed.

Table 1. Summary of Image Analysis Key Indicators.

Writing Speed	Average Width	Width Std.	Top Edge Std.	Bottom Edge Std.
10 (mm/s)	293 µm	5 µm (1.70%)	6 µm (2.05%)	7 µm (2.39%)
25 (mm/s)	239 µm	8 µm (3.34%)	11 µm (4.60%)	10 µm (4.18%)
50 (mm/s)	235 µm	9 µm (3.83%)	13 µm (5.53%)	13 µm (5.53%)
75 (mm/s)	237 µm	7 µm (2.95%)	13 µm (5.49%)	15 µm (6.33%)
100 (mm/s)	228 µm	8 µm (3.51%)	7 µm (3.07%)	8 µm (3.51%)

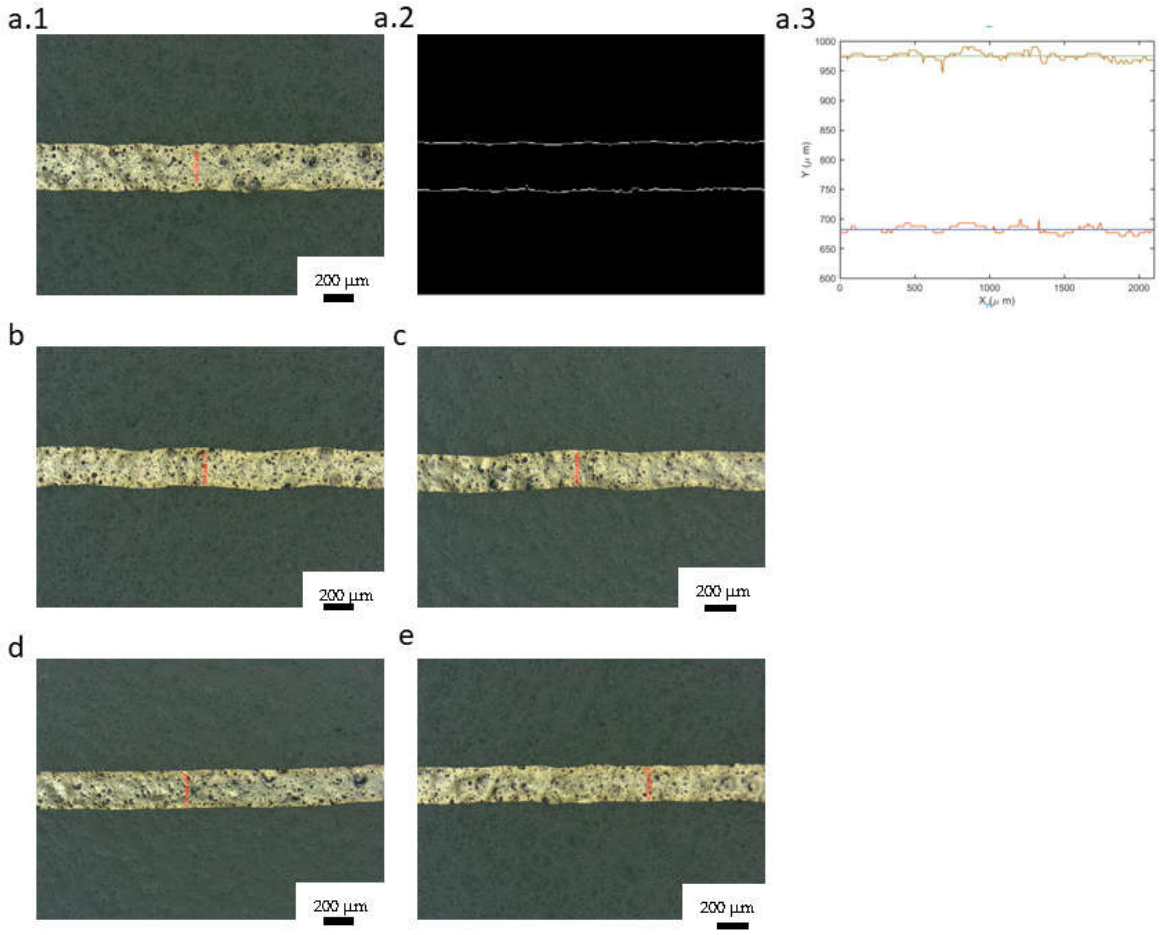

Figure 2. Microscope images depicting single lines drawn at various speeds (**a.1**) 10 mm/s, (**b**) 25 mm/s, (**c**) 50 mm/s, (**d**) 75 mm/s, and **(e)** 100 mm/s. Panels (**a.2**) and (**a.3**) depict two of the main stages for the digitization of the image data.

Since contacting pads are essential building blocks of every circuit, we also studied different hatching strategies when drawing contact squares and lines (Figure 3). Each area consists of two pass overs with different angle combinations of 90° and 45°. The worst case is found for hatching performed with perpendicular lines, where the pads are not fully covered. For the other combinations, there is no significant changes. Looking at these results, it is feasible to produce IDEs with 240 µm with about the same interspacing among fingers, which are common dimensions in printed IDEs for sensing applications [35–37].

The main driver in achieving uniform printing without bulging or breaking of the area with a single pass is the inter-line spacing. The approach can be derived from the theory of ink-jet printing, where studies have been carried out to calculate the maximum droplet spacing allowed—i.e., for a given contact angle between the ink and the substrate—to guarantee a continuous line. It can be shown that the instability threshold for moderately hydrophilic substrates (i.e., with contact angle below 70°) is at circa 90% of the droplet spherical size. In other words, in order to have continuous lines, it is necessary to have at least a marginal overlapping between droplets [38].

In this avenue, we based our choice of parameters on the fact that in order to have gapless surfaces, the lines would have a marginal overlap. Consistent with the findings in previous ink-jet printing theory, we observed that a line spacing of 90% of the line width would allow us to cover areas without gaps (Figure 3). The final results with these patterns are virtually indistinguishable from more complex patterns because the angled crosshatch (Figure 3d,e) resulted in significantly higher quantities of released ink and writing time.

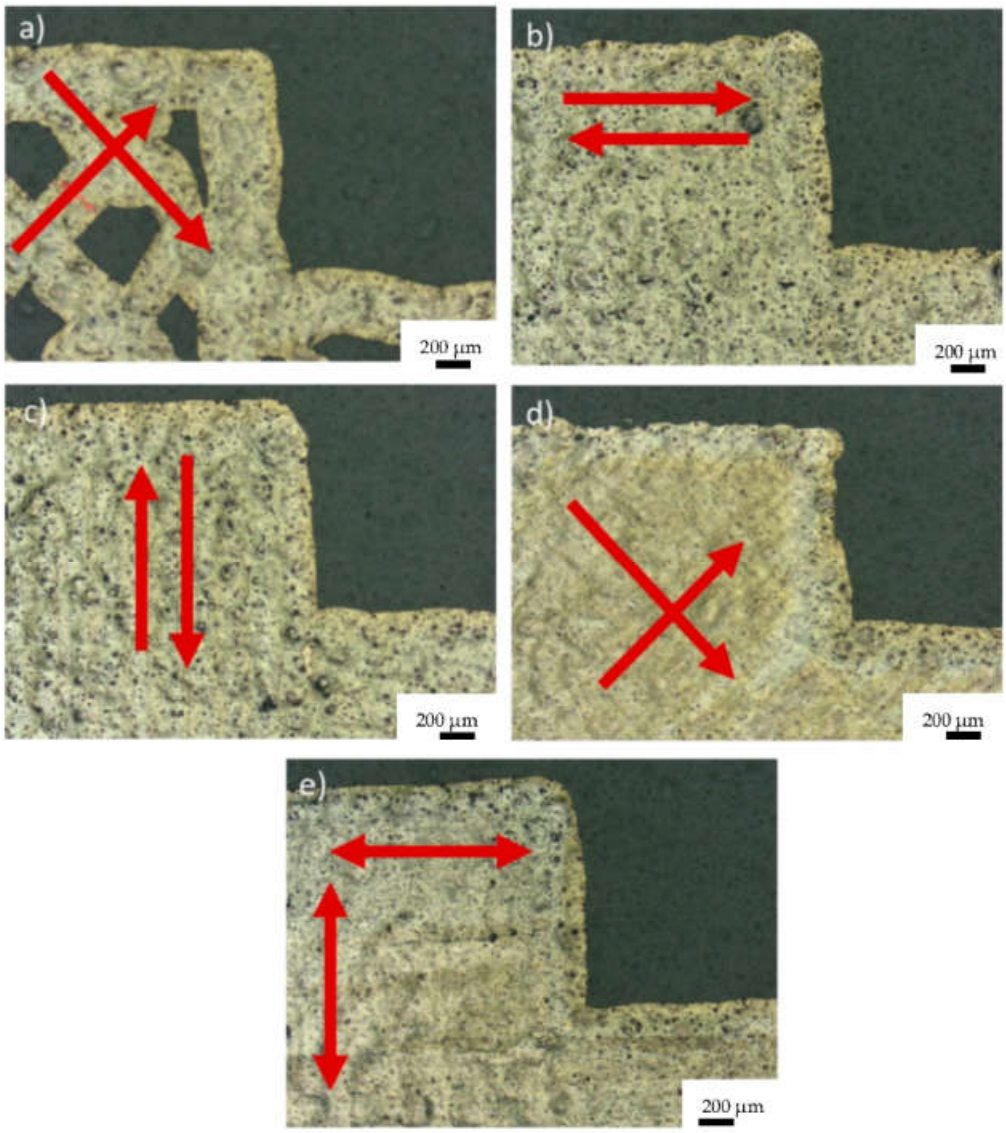

Figure 3. Microscope images depicting resulting contact pads and lines drawn with different hatching strategies. Each area consists of two pass overs: (**a**) incomplete hatching with hatchspace 2× larger than line width at 90°; (**b**) parallel horizontal lines with hatchspacing equal to 90% of line width; (**c**) parallel vertical lines with hatchspacing equal to 90% of line width; (**d**) 90° angled crosshatch at 45° configuration with hatchspacing equal to 90% of line width; (**e**) 90° angled crosshatch with hatchspacing equal to 90% of line width.

3.2. Thickness and Roughness

One essential parameter when it comes to fabrication techniques is the thickness obtained in one-step and the roughness of the resulting layer. For this purpose, we drew single lines of 250 µm at 75 mm/s.

The thickness of the AgNP-films was determined using WLI, as sketched in Figure 4, which illustrates the WLI-image for a photopaper/AgNP-film transition. The thickness of the AgNP-film yields to 164 ± 8 nm, which considers the average over 5 distinct areas of 3 µm × 3 µm on both sides, i.e., the AgNP film and the photopaper side.

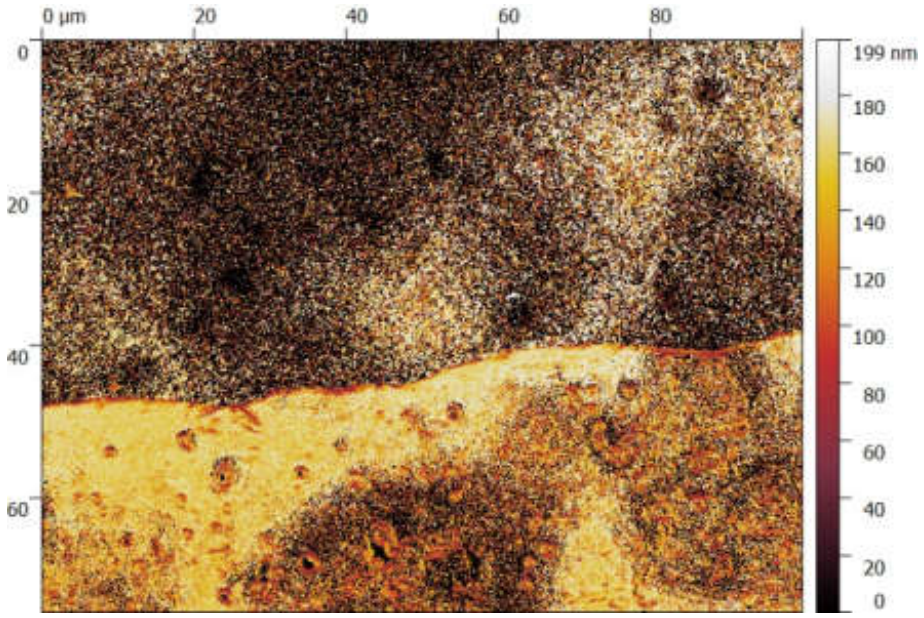

Figure 4. WLI-image for the photopaper/AgNP-film transition recorded over an area of 100 µm × 75 µm.

3.3. DC Characterization

The hatching and thickness of the printed layers can also heavily influence the conductivity of the printed films. Low sheet resistance for conductive layers offers multiple benefits in the realization of sensors' physical layers by interconnecting building blocks of sensor systems (such as antennas for RFID systems).

Both for capacitive and resistive sensors, a high resistivity of conductive lines might result in a significant loss of sensitivity, because the parasitic resistance will become more and more dominant. The response of a resistive chemosensor, for instance, can be modelled in a first approximation as:

$$R_{sensor}(c) = R_{contacts} + R_{film}(c)\Delta R_{\%}(c) = \frac{R_{film}(c)}{R_{contacts} + R_{film}(c)} \times 100$$

where R_{sensor} is the total resistance of the sensor, composed of the conductors' resistance ($R_{contacts}$) and the resistance of the sensing film ($R_{film}(c)$). Only the latter is a function of the concentration c. When printing parameters are not optimized and the resistance of the contacts becomes predominant, there would be an undesired loss of sensitivity. An analogous rationale can be followed for capacitive sensors, yet for the sake of conciseness it will not be explicitly reported here.

Additionally, the lower the interconnect resistance then the lower the losses within the printed system (a critical item for any device powered by batteries or energy harvesters), and similar considerations can be expressed for the resistivity of printed antennae.

One of the targets of the process optimization for this automated HWE technique shall then be the reduction of the sheet resistance of the written silver layers. To achieve this goal through electrical characterization of the silver patterns, we studied the sheet resistance of the written patterns obtained at 75 mm/s, which are illustrated in Figure 5. The mean value is about 550 mΩ/sq. However, this value can be reduced by almost to half (300 mΩ/sq.) by using a double 90° angle crosshatch with hatch spacing equal to 90% of line width.

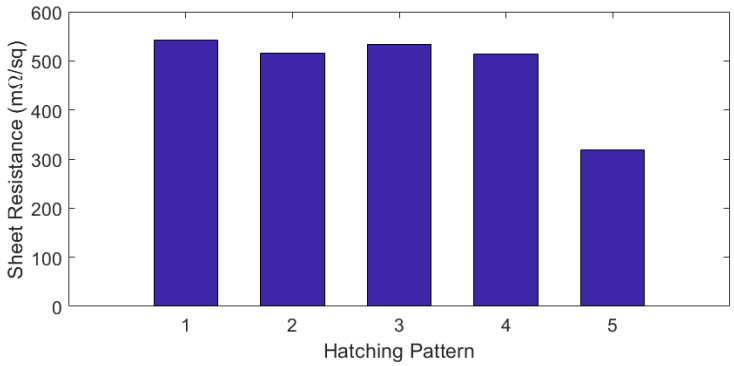

Figure 5. Relationship between hatching pattern and sheet resistance. (1) Parallel horizontal lines with hatchspacing equal to 90% of line width. (2) Parallel vertical lines with hatchspacing equal to 90% of line width. (3) 90° angled crosshatch at 45° configuration with hatchspacing equal to 90% of line width. (4) 90° angled crosshatch with hatchspacing equal to 90% of line width. (5) Double 90° angled crosshatch with hatchspacing equal to 90% of line width.

The average thickness of the silver layer was circa 165 nm; however, the hatching pattern significantly affects the sheet resistance due to the route taken by the pen, and consequently the way in which the particles agglomerate and the total amount of material deposited on the substrate.

3.4. Applications

We employed a technique used to fabricate electronic devices that normally belongto the PE domain rather than to the HWE, because of the low degree of control that normally can be obtained with handwriting methods. In particular, we used this procedure to fabricate IDEs on paper for gas sensors (see Figure 6a), which are characterized in [39], and radiofrequency identification (RFID) tags (Figure 6b), creating two of the main building blocks of fully printed sensing systems.

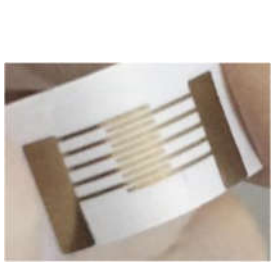

(**a**)

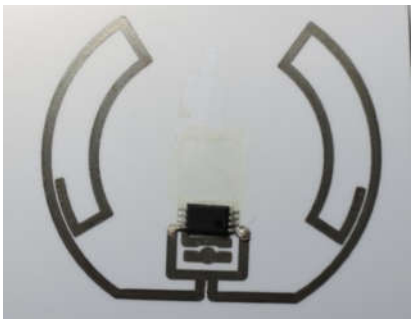

(**b**)

Figure 6. Prototypes developed with this handwriting technique: (**a**) an IDE for gas sensor; (**b**) an UHF RFID tag.

The gas sensors were composed by Ag NP electrodes written with the system here described with a finger width and interspacing of 300 µm. On top of the IDEs, a carbon nanotube (CNT) layer was also written, which acts as sensing layer. Such sensor exhibited sensitivities similar to other CNT-based resistive sensors [40–42].

The response with respect to NH_3 (shown in Figure 7) is in line in terms of relative changes, time constants and general behaviour with what we described in our previous works, where similar material stacks were deposited with different technologies. In particular, it can be observed the characteristic resistance drop when the sensor is heated, followed by a recovery trend to the initial resistance value, and different slopes and growth of the resistance as a function of the gas concentration.

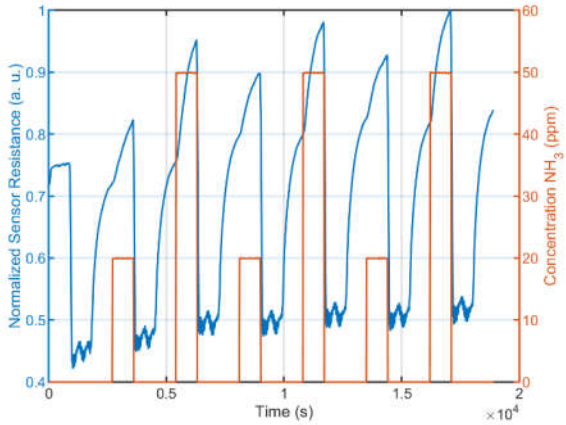

Figure 7. Response, in terms of normalized resistance, to the exposure of the sensor to two different concentrations of NH_3. The sensor undergoes cycles of heating, thermal recovery and exposure to concentrations of 20 ppm and 50 ppm of HN_3.

We also manufactured a RFID tag on paper, which is essential for the read-out of autonomous systems. The tag operates in the ultrahigh frequency (UHF) band. The employed the chip EM4325 (from EM Microelectronic) with the optimized antenna provided by this manufactured (see Figure 6b) with a diameter of 3.8 cm. The total length of the dipole arms is 8.6 cm. The antenna is designed to resonate at 867 MHz. We checked the RFID tag with a commercial reader (DK-UHF RFID HP2 from IDS Microchip AG, Switzerland), and we only achieved a reading range of 0.4 m, which is sub-optimal when compared to commercial antennae, but it could be sufficient for most practical applications. Although the antenna is functional, it suffers from the inherit high resistance of the printed pattern. The values obtained in this work (in the order of hundreds of mΩ/sq.) compared to other printed antennas, such as the inkjet printed ones (sheet resistance in the order of tens of mΩ/sq.), are indeed about an order of magnitude higher with an optimized photonic sintering process [34]. Nevertheless, in case longer reading distances are required, this shortcoming can be overcome by printing thicker patters (increasing the number of printed layers [43]) or enhancing conductivity by the tuning/selection of the used conductive ink.

Both gas sensors and RFID tags are key pillars in the development of the IoT, which is of great interests if both cost-effective manufacturing process and biodegradable materials like paper are employed.

Regarding the cost of the described automated HWE, the total cost of the system is below 500 €. The robot is about 450 € and the pen with reservoir is around 20 €, which can be reutilized several times if it is properly cleaned. This total cost is much lower than almost any dedicated printing equipment for electronics and cheaper than almost any printing system. Moreover, the cost of empty reservoir is about 2 €, which is much cheaper than any consumable of other printing system.

4. Conclusions

In this work, we studied an automatized handwriting technique based on ball pens. We benchmarked and tested for prototyping different printed electronic devices, aiming to demonstrate the feasibility of handwritten complex sensing systems.

It was found that the best compromise between the straightness of lines and desired width was 75 mm/s. Further, the hatching patterns reduced the sheet resistance of the produced layouts. In particular, a double 90° angled crosshatch with hatchspacing equal to 90% of line width decreased the obtained sheet resistance in half, with respect to the other hatching patterns analyzed. However, they did not show any apparent difference in terms of morphology and coverage level. Using these optimal parameters of speed and hatching pattern, this technique reproduced patterns with a resolution of 250 μm and sheet resistance of about 300 mΩ/sq.

Reproducibility was good enough to manufacture similar conductive patterns with errors below 3%, which is a key finding for the production of reliable sensors with repeatable characteristics and antennae with predictive performance.

Such a technique has been employed to fabricate and test printed electrodes for gas sensors and RFID antennas at the HF band. The described technology paves the way for DIY in-house prototyping and for "decorative" electronic nodes, where accurate handwritten patterns can be used to disguise the presence of a sensor or antenna. Compared to other printing techniques, two advantages can be highlighted: due to the additive fabrication process, which impies no waste of materials, and the ultra-low-cost equipment that minimizes both, the time and cost associated with the produced sustainable electronic prototypes. This fact can be important in iterative design processes, where slightly different prototypes need to be fabricated until the optimal design is reached like in the case of antenna design and where antenna performance is optimized through small differences in the design. The limitations of the proposed technique are related to the lower performance compared to other comparable fabrication techniques (e.g., inkjet printing), although they can be overcome by depositing multiple layers (in an approach similar to what ink-jet printing or spray-deposition employ).

In this work, we focused on the optimization of writing conductive silver; we demonstrated the utilization of the same technique with carbon nanotubes in a previous work. Therefore, this technique is versatile and can be utilized with various materials to manufacture complete sensing tags by just filling the pen with another cartridge.

Author Contributions: Conceptualization, A.F. and A.R.; methodology, F.C.L.; validation, F.C.L. and J.F.S.; resources, M.B.; writing—original draft preparation, A.F. and A.R.; writing—review and editing, J.F.S.; supervision, P.L. All authors have read and agreed to the published version of the manuscript.

Funding: This work was supported by the TUM Graduate School and by the European Commission through the fellowship H2020-MSCA-IF-2017-794885-SELFSENS.

Institutional Review Board Statement: Not applicable.

Informed Consent Statement: Not applicable.

Data Availability Statement: Data are available upon request.

Conflicts of Interest: The authors declare no conflict of interest.

References

1. Miorandi, D.; Sicari, S.; De Pellegrini, F.; Chlamtac, I. Internet of things: Vision, applications and research challenges. *Ad. Hoc. Netw.* **2012**, *10*, 1497–1516. [CrossRef]
2. Perera, C.; Liu, C.H.; Jayawardena, S. The emerging internet of things marketplace from an industrial perspective: A survey. *IEEE Trans. Emerg. Top. Comput.* **2015**, *3*, 585–598. [CrossRef]
3. Perelaer, J.; Smith, P.J.; Mager, D.; Soltman, D.; Volkman, S.K.; Subramanian, V.; Korvink, J.G.; Schubert, U.S. Printed electronics: The challenges involved in printing devices, interconnects, and contacts based on inorganic materials. *J. Mater. Chem.* **2010**, *20*, 8446–8453. [CrossRef]
4. Suganuma, K. *Introduction to Printed Electronics*; Springer Science & Business Media: Berlin/Heidelberg, Germany, 2014; Volume 74.
5. Cantatore, E. Applications of organic and printed electronics. In *A Technology-Enabled Revolution*; Springer Science + Business Media: New York, NY, USA, 2013; p. 180.
6. Li, Z.; Liu, H.; Ouyang, C.; Hong Wee, W.; Cui, X.; Jian Lu, T.; Pingguan-Murphy, B.; Li, F.; Xu, F. Recent Advances in Pen-Based Writing Electronics and their Emerging Applications. *Adv. Funct. Mater.* **2016**, *26*, 165–180. [CrossRef]
7. Rivadeneyra, A.; López-Villanueva, J.A. Recent Advances in Printed Capacitive Sensors. *Micromachines* **2020**, *11*, 367. [CrossRef]
8. Romero, F.J.; Rivadeneyra, A.; Salinas-Castillo, A.; Ohata, A.; Morales, D.P.; Becherer, M.; Rodriguez, N. Design, fabrication and characterization of capacitive humidity sensors based on emerging flexible technologies. *Sens. Actuators B Chem.* **2019**, *287*, 459–467. [CrossRef]
9. Alkin, K.; Stockinger, T.; Zirkl, M.; Stadlober, B.; Bauer-Gogonea, S.; Kaltenbrunner, M.; Bauer, S.; Müller, U.; Schwödiauer, R. Paper-based printed impedance sensors for water sorption and humidity analysis. *Flex. Print. Electron.* **2017**, *2*, 014005. [CrossRef]

10. Colella, R.; Chietera, F.; Catarinucci, L.; Salmeron, J.; Rivadeneyra, A.; Carvajal, M.; Palma, A.; Capitán-Vallvey, L. Fully 3D-Printed RFID Tags based on Printable Metallic Filament: Performance Comparison with other Fabrication Techniques. In Proceedings of the 2019 IEEE-APS Topical Conference on Antennas and Propagation in Wireless Communications (APWC), Granada, Spain, 9–13 September 2019; pp. 253–257.
11. Colella, R.; Rivadeneyra, A.; Palma, A.J.; Tarricone, L.; Capitan-Vallvey, L.F.; Catarinucci, L.; Salmeron, J.F. Comparison of Fabrication Techniques for Flexible UHF RFID Tag Antennas [Wireless Corner]. *IEEE Antennas Propag. Mag.* **2017**, *59*, 159–168. [CrossRef]
12. Ishida, K.; Huang, T.-C.; Honda, K.; Shinozuka, Y.; Fuketa, H.; Yokota, T.; Zschieschang, U.; Klauk, H.; Tortissier, G.; Sekitani, T. Insole pedometer with piezoelectric energy harvester and 2 V organic circuits. *IEEE J. Solid-State Circuits* **2013**, *48*, 255–264. [CrossRef]
13. Chang, J.; Zhang, X.; Ge, T.; Zhou, J. Fully printed electronics on flexible substrates: High gain amplifiers and DAC. *Org. Electron.* **2014**, *15*, 701–710. [CrossRef]
14. Kurra, N.; Dutta, D.; Kulkarni, G.U. Field effect transistors and RC filters from pencil-trace on paper. *Phys. Chem. Chem. Phys.* **2013**, *15*, 8367–8372. [CrossRef]
15. Lin, C.-W.; Zhao, Z.; Kim, J.; Huang, J. Pencil drawn strain gauges and chemiresistors on paper. *Sci. Rep.* **2014**, *4*, 1–6. [CrossRef] [PubMed]
16. Gao, Y.; Li, H.; Liu, J. Direct writing of flexible electronics through room temperature liquid metal ink. *PLoS ONE* **2012**, *7*, e45485. [CrossRef]
17. Russo, A.; Ahn, B.Y.; Adams, J.J.; Duoss, E.B.; Bernhard, J.T.; Lewis, J.A. Pen-on-paper flexible electronics. *Adv. Mater.* **2011**, *23*, 3426–3430. [CrossRef]
18. Han, Y.L.; Hu, J.; Genin, G.M.; Lu, T.J.; Xu, F. BioPen: Direct writing of functional materials at the point of care. *Sci. Rep.* **2014**, *4*, 4872. [CrossRef]
19. Han, J.-W.; Kim, B.; Li, J.; Meyyappan, M. Carbon nanotube ink for writing on cellulose paper. *Mater. Res. Bull.* **2014**, *50*, 249–253. [CrossRef]
20. Warren, H.; Gately, R.D.; Moffat, H.N. Conducting carbon nanofibre networks: Dispersion optimisation, evaporative casting and direct writing. *RSC Adv.* **2013**, *3*, 21936–21942. [CrossRef]
21. He, J.; Luo, M.; Hu, L.; Zhou, Y.; Jiang, S.; Song, H.; Ye, R.; Chen, J.; Gao, L.; Tang, J. Flexible lead sulfide colloidal quantum dot photodetector using pencil graphite electrodes on paper substrates. *J. Alloy. Compd.* **2014**, *596*, 73–78. [CrossRef]
22. Gimenez, A.J.; Yanez-Limon, J.; Seminario, J.M. ZnO− paper based photoconductive UV sensor. *J. Phys. Chem. C* **2010**, *115*, 282–287. [CrossRef]
23. ul Hasan, K.; Nur, O.; Willander, M. Screen printed ZnO ultraviolet photoconductive sensor on pencil drawn circuitry over paper. *Appl. Phys. Lett.* **2012**, *100*, 211104. [CrossRef]
24. Mirica, K.A.; Weis, J.G.; Schnorr, J.M.; Esser, B.; Swager, T.M. Mechanical drawing of gas sensors on paper. *Angew. Chem. Int. Ed.* **2012**, *51*, 10740–10745. [CrossRef]
25. Frazier, K.M.; Mirica, K.A.; Walish, J.J.; Swager, T.M. Fully-drawn carbon-based chemical sensors on organic and inorganic surfaces. *Lab Chip* **2014**, *14*, 4059–4066. [CrossRef]
26. Gao, Y.; Li, H.; Liu, J. Directly writing resistor, inductor and capacitor to composite functional circuits: A super-simple way for alternative electronics. *PLoS ONE* **2013**, *8*, e69761. [CrossRef] [PubMed]
27. Li, W.; Chen, M. Synthesis of stable ultra-small Cu nanoparticles for direct writing flexible electronics. *Appl. Surf. Sci.* **2014**, *290*, 240–245. [CrossRef]
28. Devi, K.C.; Angadi, B.; Mahesh, H. Multiwalled carbon nanotube-based patch antenna for bandwidth enhancement. *Mater. Sci. Eng. B* **2017**, *224*, 56–60. [CrossRef]
29. Li, Z.; Li, F.; Hu, J.; Wee, W.H.; Han, Y.L.; Pingguan-Murphy, B.; Lu, T.J.; Xu, F. Direct writing electrodes using a ball pen for paper-based point-of-care testing. *Analyst* **2015**, *140*, 5526–5535. [CrossRef]
30. Kano, S.; Fujii, M. All-painting process to produce respiration sensor using humidity-sensitive nanoparticle film and graphite trace. *ACS Sustain. Chem. Eng.* **2018**, *6*, 12217–12223. [CrossRef]
31. Yu, Y.; Zhang, J.; Liu, J. Biomedical implementation of liquid metal ink as drawable ECG electrode and skin circuit. *PLoS ONE* **2013**, *8*, e58771. [CrossRef] [PubMed]
32. Liu, Y.; Mo, S.; Shang, S.; Wang, P.; Zhao, W.; Li, L. Handwriting flexible electronics: Tools, materials and emerging applications. *J. Sci. Adv. Mater. Devices* **2020**, *5*, 451–467. [CrossRef]
33. Soum, V.; Cheong, H.; Kim, K.; Kim, Y.; Chuong, M.; Ryu, S.R.; Yuen, P.K.; Kwon, O.-S.; Shin, K. Programmable Contact Printing Using Ballpoint Pens with a Digital Plotter for Patterning Electrodes on Paper. *Acs Omega* **2018**, *3*, 16866–16873. [CrossRef]
34. Albrecht, A.; Rivadeneyra, A.; Abdellah, A.; Lugli, P.; Salmerón, J.F. Inkjet printing and photonic sintering of silver and copper oxide nanoparticles for ultra-low-cost conductive patterns. *J. Mater. Chem. C* **2016**, *4*, 3546–3554. [CrossRef]
35. Rivadeneyra, A.; Bobinger, M.; Albrecht, A.; Becherer, M.; Lugli, P.; Falco, A.; Salmerón, J.F. Cost-effective PEDOT: PSS Temperature Sensors Inkjetted on a Bendable Substrate by a Consumer Printer. *Polymers* **2019**, *11*, 824. [CrossRef] [PubMed]
36. Loghin, F.C.; Falco, A.; Salmeron, J.F.; Lugli, P.; Abdellah, A.; Rivadeneyra, A. Fully transparent gas sensor based on Carbon Nanotubes. *Sensors* **2019**, *19*, 4591. [CrossRef] [PubMed]

37. Abdelhalim, A.; Winkler, M.; Loghin, F.; Zeiser, C.; Lugli, P.; Abdellah, A. Highly sensitive and selective carbon nanotube-based gas sensor arrays functionalized with different metallic nanoparticles. *Sens. Actuators B Chem.* **2015**, *220*, 1288–1296. [CrossRef]
38. Moon, Y.J.; Kang, H.; Lee, S.H.; Kang, K.; Cho, Y.J.; Hwang, J.Y.; Moon, S.J. Effect of contact angle and drop spacing on the bulging frequency of inkjet-printed silver lines on FC-coated glass. *J. Mech. Sci. Technol.* **2014**, *28*, 1441–1448. [CrossRef]
39. Loghin, F.C.; Falco, A.; Albrecht, A.; Salmerón, J.F.; Becherer, M.; Lugli, P.; Rivandeneyra, A. A Handwriting Method for Low-Cost Gas Sensors. *ACS Appl. Mater. Interfaces* **2018**, *10*, 34683–34689. [CrossRef]
40. Abdelhalim, A.; Falco, A.; Loghin, F.; Lugli, P.; Salmerón, J.F.; Rivadeneyra, A. Flexible NH3 sensor based on spray deposition and inkjet printing. In Proceedings of the SENSORS, 2016 IEEE, Orlando, FL, USA, 30 October–3 November 2016; pp. 1–3.
41. Falco, A.; Rivadeneyra, A.; Loghin, F.C.; Salmerón, J.F.; Lugli, P.; Abdelhalim, A. Towards Low-Power Electronics: Self-Recovering and Flexible Gas Sensors. *J. Mater. Chem. A* **2018**, *6*, 7107–7113. [CrossRef]
42. Eising, M.; Cava, C.E.; Salvatierra, R.V.; Zarbin, A.J.G.; Roman, L.S. Doping effect on self-assembled films of polyaniline and carbon nanotube applied as ammonia gas sensor. *Sens. Actuators B Chem.* **2017**, *245*, 25–33. [CrossRef]
43. Salmerón, J.F.; Molina-Lopez, F.; Briand, D.; Ruan, J.J.; Rivadeneyra, A.; Carvajal, M.A.; Capitán-Vallvey, L.; de Rooij, N.F.; Palma, A.J. Properties and Printability of Inkjet and Screen-Printed Silver Patterns for RFID Antennas. *J. Electron. Mater.* **2014**, *43*, 604–617. [CrossRef]